Finite Element Simulation of Pre-Heating Effect on Melt Pool Size During Micro-Plasma Transferred Arc Deposition Process

Sagar H Nikam[1, *] and Neelesh K Jain[2]

[1]Research Scholar, Discipline of Mechanical Engineering, Indian Institute of Technology Indore, Simrol 453 552 (MP) India.
[2]Professor, Discipline of Mechanical Engineering, Indian Institute of Technology Indore, Simrol 453 552 (MP) India.

*Corresponding author: sagariiti@gmail.com

Abstract. This paper reports on simulating the effect of substrate pre-heating on melt pool size during deposition of titanium alloy (Ti-6Al-4V) on the similar substrate material using micro-plasma transferred arc (μ-PTA) deposition process. It involved (i) three-dimensional finite element simulation (3D-FES) of pre-heating of Ti-6Al-4V substrate material within the range of 400-450 K using furnace, (ii) simulating the formation of melt pool on the pre-heated and non-heated substrate material along μ-PTA torch movement and (iii) image processing of the melt pool to predict its width and depth obtained by μ-PTA deposition process. Obtained results revealed that (i) pre-heated substrate exhibited good distribution of temperature as compared to substrate exposed to ambient temperature and (ii) increase in melt pool width and depth has been observed for pre-heated substrate as compared to melt pool formed at ambient temperature which reveals that pre-heated substrate can be effectively used for depositing titanium alloy.

1. Introduction

Titanium alloys (Ti-6Al-4V) is high strength, high toughness, excellent temperature toughness and high resistance to corrosion material used for manufacturing aircraft structures, engines and bio-medical components. Due to complexity in manufacturing these components, alternative bottom-up approach of manufacturing known as Additive layer manufacturing (ALM) process can be used. However, titanium alloy possesses relatively lower thermal conductivity as compared to other metals, which make it difficult to use in ALM processes. Therefore, most of the researcher have used titanium alloy material with high energy beam (i.e. laser and electron) and arc (i.e. gas metal arc, metal inert gas etc.) based ALM processes.

Titanium alloy (Ti6-6Al-4V) material in wire form was used for manufacturing components using Nd:YAG laser based deposition process [1]. While its mechanical properties such as tension and fatigue tests were done on the layer manufactured components [2]. Lasers were further used for depositing titanium alloy in closed container using selective laser sintering method. In this process, bed of titanium alloy powder was spread inside the sealed container and then the beam was moved over the selected areas doing multi-layer deposition [3]. Electron beam melting has been used for depositing wrought Ti-6Al-4V alloy material for biomedical applications. Performance of

manufactured bio-medical components were analysed by conducting tensile test and Vickers hardness test [4]. In arc based processes, tungsten inert gas welding process was used for deposition of titanium alloy. In this study, effect of process parameter on deposition morphology has been investigated [5]. Further, plasma arc welding based ALM was used to build a 3D structure using titanium alloy in wire form. Suitability of this deposition process was investigated by using this process for manufacturing large aerospace components [6].

It has been observed from past literature that, to obtain good strength for layer manufactured components using Ti-6Al-4V, good bonding between each successive layer is required which is mainly dependent on the melt pool formed by the heat source during deposition. However, formation of melt pool is easy in high energy beam and arc based processes, but it becomes difficult when titanium alloy is used for micro-energy arc based processes like micro-plasma transferred arc based deposition process. Therefore, present work aims to develop (i) 3D-FES of pre-heating of Ti-6Al-4V substrate material within the range of 400-450 K using furnace, (ii) Simulating the formation of melt pool along µ-PTA torch movement on the non-heated and pre-heated substrate material and (iii) predict the melt pool width and depth using image processing technique.

2. Simulation

Simulation of melt pool for µ-PTA process was done using ANSYS (version 17.2) software [7].

2.1. Assumptions

- Constant distance is maintained between micro-plasma torch and substrate.
- Geometry of the melt pool remains constant along µ-PTA torch movement direction.

2.2. Governing equation

Micro-plasma transferred arc is a thermal process in which heat conduction is the dominant mode of heat transfer. Therefore, heat conduction governing equation written as follows has been used in present work [8].

$$\rho_s C_{ps}\left(\frac{\partial T}{\partial t}\right) = q + \nabla \cdot (K_s^* \nabla T) + \nabla Q_f \quad (1)$$

In which, ρ_s is the substrate material density (Kg/m^3); C_{ps} is the substrate material specific heat (J/Kg K); t is the micro-plasma arc time (s); q is the actual density of heat flux of micro-plasma arc (W/m^3); T is melt pool temperature (K); K_s* is the modified substrate material thermal conductivity for Marangoni flow (W/m K) and Q_f is the density of heat flux of furnace (W/m^2).

- **Initial condition:** Ambient temperature condition. i.e.

$$T(x, y, z, t) = T_i \quad (2)$$

  Where, T_i (K) is the ambient temperature.
- **Pre-heating Condition:** This condition was given to the elements associated with external areas of the substrate material in the form of heat flux. Where the external surface of substrate material was constant heated using furnace operated at 500 W for 240 secs until the substrate material gets heated between 400 to 450 K.
- **Heat source model:** In the present work, Gaussian heat source model modified by considering current density *'J'* (A/m^2) in µ-plasma arc and electric field *'E'* (V/m) has been used [8]. Theoretic density of heat flux *q(x,y)* value obtained at *x* and *y* coordinates considering center of micro-plasma arc radius *'r_o'* is calculated as follows

$$q(x, y) = J\, E\, exp^{\frac{-(x^2+y^2)}{r_o^2}} \quad (3)$$

Here, the micro-plasma current density *'J'* is calculated by multiplying electrical conductivity *'σ_{es}'* of the substrate material as 5.8 x 10^5 ohm^{-1}m^{-1} with electric field on the substrate material 'E_{es}'. It is considered approximately equal to electric field *'E'* (i.e. =V/L, Where, *V* is the arc voltage of micro-plasma in volts and *L* is the space maintained between nozzle and substrate)

$$J \approx \sigma_{es}\, E_{es} \approx \sigma_{es} \frac{V}{L} \quad Where\ E_{es} \sim E \tag{4}$$

Actual density of heat flux of micro-plasma arc *'q'* (W/m^3) was obtained by multiplying theoretic density of heat flux *'q(x,y)'* with its thermal efficiency *'η'*

$$q = \eta\, q(x,y) \tag{5}$$

Thermal efficiency *'η'* value as 60% is considered [8].

- **Marangoni flow:** Its influence was considered by modifying substrate material thermal conductivity [9] given as follows

$$K_s^* = CK_s \quad if\ T > T_{ms} \tag{6}$$

Where, *C* is the factor of correction (= 2.5 is used in present study); K_s* is the substrate material thermal conductivity modified for Marangoni flow (W/m K) and K_s is the substrate material thermal conductivity (W/m K).

- **Heat loss from the substrate material:** It can be described as follows

$$(K_s^* \nabla T) \cdot n = \varepsilon_s\, \sigma_{sbc}(T_{ms}^4 - T_i^4) + h_{conv}(T_{ms} - T_i) \tag{7}$$

Here, ε_s is the emissivity of the substrate material; σ_{sbc} is the Stefan-Boltzmann constant (5.67 x 10^{-8} W/m^2 K^4); T_{ms} is melting temperature of the substrate material (K); h_{conv} is the coefficient of convective heat transfer (W/m^2 K).

- **Temperature-dependent material properties:** Figure 1 depicts the distribution of specific heat (Figure 1a); thermal conductivity (Figure 1b) and density (Figure 1c) of the substrate material (i.e. titanium alloy Ti-6Al-4V) with temperature.

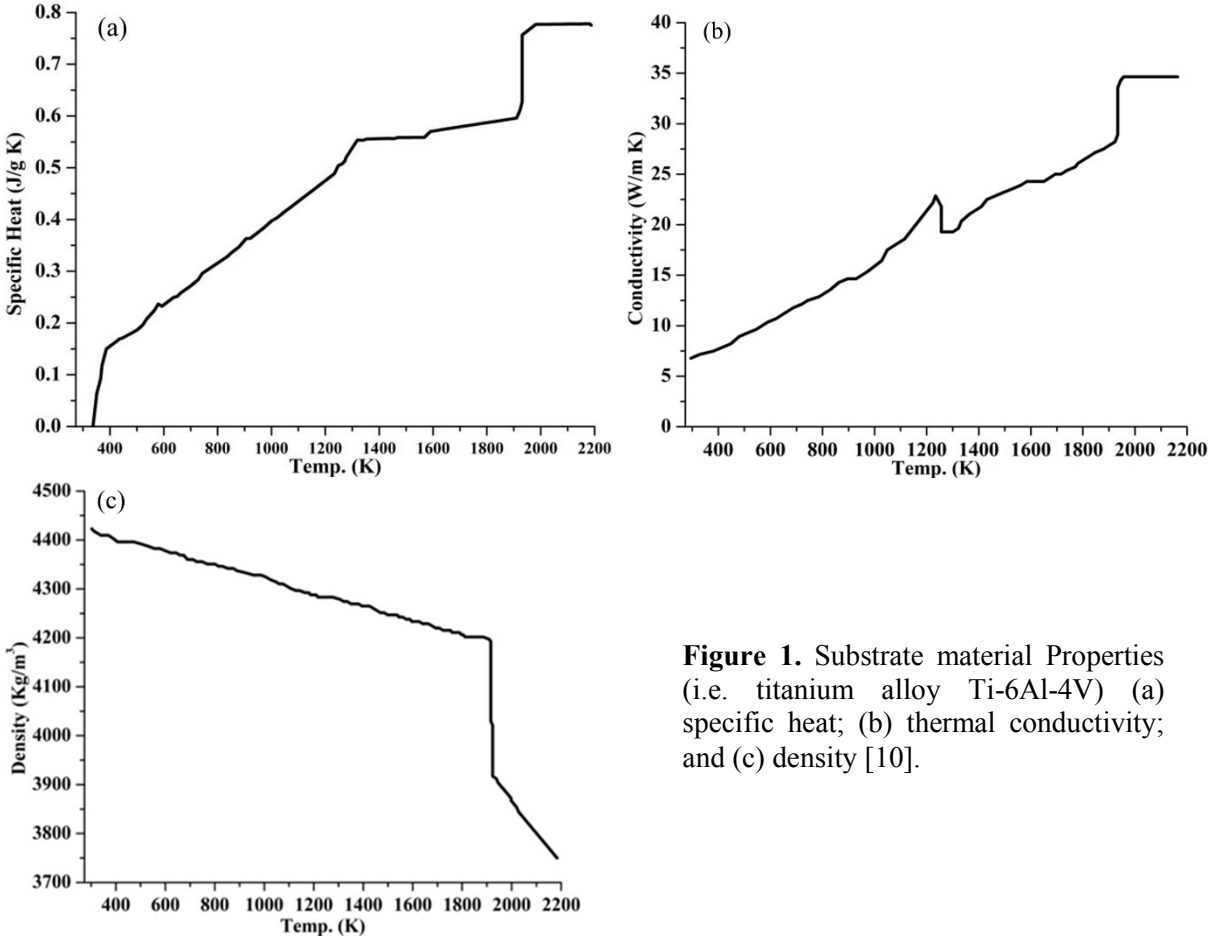

Figure 1. Substrate material Properties (i.e. titanium alloy Ti-6Al-4V) (a) specific heat; (b) thermal conductivity; and (c) density [10].

- **Melt pool simulation:** For present work, temperature distribution is simulated within melt pool created during μ-PTA deposition process on non-heated and pre-heated substrate material.

Simulation was done on substrate material of Ti-6Al-4V, its dimensions as 50 mm × 25 mm × 3 mm were considered. Micro-plasma power as 460 W and torch travel rate as 100 mm/min was used in present simulation. Substrate material geometry was discretized with 8-node cubic elements with an edge length of 0.025 mm as shown in Figure 2. In the ANSYS [7] software, element type SOLID70 was used for 3D-FES of melt pool. Micro-plasma torch movement direction is along y-axis.

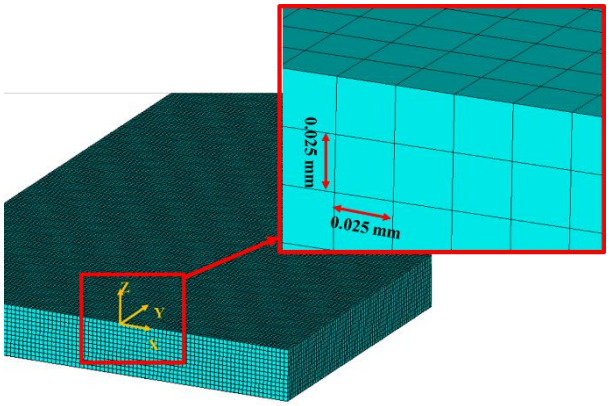

Figure 2. Substrate geometry meshed for 3D-FES of melt pool.

3. Result and discussion

3.1. Temperature distribution analysis

Figure 3 presents distribution of temperature in the melt pool formed in non-heated (Figure 3a) and pre-heated (Figure 3b) substrate material of Ti-6Al-4V during µ-PTA deposition process. It can be observed from Figure 3a that, the temperature distribution is constrained within the substrate material when it is at ambient temperature. While Figure 3b depicts unconstrained temperature distribution within the substrate material. The results revealed that, due to low thermal conductivity of titanium alloy the flow of heat within non-heated substrate material is restricted while due to pre-heated substrate the flow of heat from substrate to atmosphere is easily relieved. Also, the heat affected zone (HAZ) around the area of melt pool in pre-heated substrate is gradually expanding as compared HAZ around melt pool in non-heated substrate. This is due to increase in heat losses by convection and radiation and increase in heat accumulation in the molten pool zone for pre-heated substrate material. From obtained results it can be concluded that pre-heated substrate exhibited good distribution of temperature as compared to substrate exposed to ambient temperature.

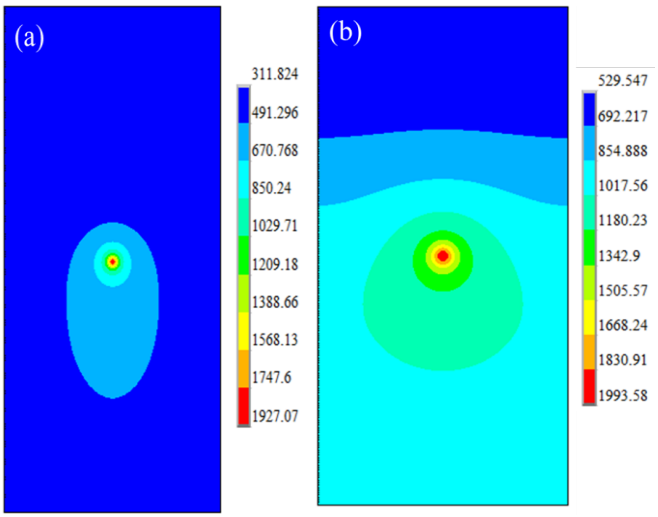

Figure 3. Distribution of temperature in the melt pool formed in (a) non-heated and (b) pre-heated substrate material.

3.2. Measurement and comparison of melt pool width and depth

Melt pool width and depth formed in the substrate material were predicted by image processing technique [11]. Images of temperature distribution obtained by finite element simulation were captured and exported to MATLAB for processing the melt pool images. Processing of the images were done by using following steps:

i) Pixels were counted for width and height of the substrate material as shown in table 1.
ii) Pixels were counted within melt pool to determine its width and depth as shown in table 1.

Table 1. Parameters used for image processing of melt pool.

Parameters	**Non-heated substrate material**	**Pre-heated substrate material**
Width of the substrate material *'s_w'*	25 mm	25 mm
Height of the substrate material *'s_h'*	3 mm	3 mm
Pixels within width of melt pool *'P_{mw}'*	10.98	27.95
Pixels within depth of melt pool *'P_{md}'*	4.97	13.88
Pixels within width of the substrate material *'P_{sw}'*	616	616
Pixels within height of the substrate material *'P_{sh}'*	73	73

Therefore, using values from table 1, melt pool width *'w_m'* for non-heated and pre-heated substrate material were calculated by using following equation

$$w_m = \frac{P_{mw} \times s_w}{P_{sw}} \tag{8}$$

Where, P_{mw} is the pixels counted for melt pool width; P_{sw} is the pixels counted for substrate width and s_w is the width of substrate material (mm). While melt pool depth *'d_m'* has been calculated by using following equation

$$d_m = \frac{P_{md} \times s_h}{P_{sh}} \tag{9}$$

Where, P_{md} is the pixels within the melt pool depth; P_{sh} is the pixels within substrate height and s_h is the height of substrate material (mm).

Figure 4 depicts the processing of the images done for predicting melt pool width (using equation 8) and depth (using equation 9) for non-heated (Figure 4a) and pre-heated (Figure 4b). Its value calculated for non-heated substrate material are 0.45 mm and 0.21 mm respectively and for pre-heated substrate material are 1.13 mm and 0.57 mm respectively. Therefore, results revealed that, increase in the melt pool width and depth has been observed for pre-heated substrate as compared to melt pool formed at ambient temperature. Therefore, pre-heated substrate material of titanium alloy can be effectively used for micro-plasma based additive layer manufacturing.

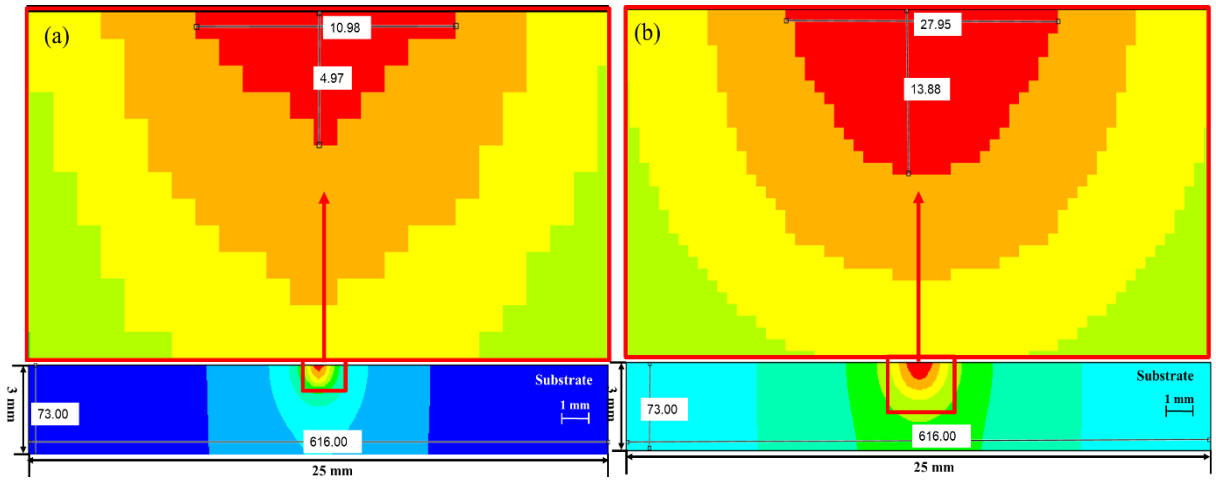

Figure 4. Image processing of melt pool formed in (a) non-heated and (b) pre-heated substrate.

4. Conclusion

This paper reported on simulating the effect of pre-heating on melt pool size using finite element simulation developed for micro-plasma transferred arc (μ-PTA) process. Temperature distribution within melt pool were studied for pre-heated and non-heated substrate material of Ti-6Al-4V. Images of simulated melt pool for both the cases were captured and exported to MATLAB for image processing to predict melt pool width and depth. Following main conclusions can be drawn from present work:

- Developed simulation can investigate the effect of pre-heating on temperature distribution within the melt pool.
- Width and depth of melt pool were predicted with good accuracy by using image processing technique.
- Pre-heated substrate of Ti-6Al-4V exhibited good distribution of temperature as compared to substrate exposed to ambient temperature.
- Increase of melt pool width and depth has been observed for pre-heated substrate as compared to melt pool formed at ambient temperature which reveals that pre-heated substrate can be effectively used for depositing titanium alloy.

References

[1] Baufeld B, Brandl E and Van der Biest O 2011 Wire based additive layer manufacturing: Comparison of microstructure and mechanical properties of Ti–6Al–4V components fabricated by laser-beam deposition and shaped metal deposition *J. Mater. Process. Tech.* **211** 1146-1158

[2] Brandl E, Baufeld B, Leyens C and Gault R 2010 Additive manufactured Ti-6Al-4V using welding wire: comparison of laser and arc beam deposition and evaluation with respect to aerospace material specifications *Phy. Proce.* **5** 595-606

[3] Roberts I A, Wang C J, Esterlein R, Stanford M and Mynors D J 2009 A three-dimensional finite element analysis of the temperature field during laser melting of metal powders in additive layer manufacturing *Int. J. Mach. Tool. Manu.* **49** 916-923

[4] Murra L E, Esquivel E V, Quinones S A, Gaytan S M, Lopez M I, Martinez E Y, Medina F, Hernandez D H, Martinez E, Martinez J L, Stafford S W, Brown D K, Hoppe T, Meyers W, Lindhe U and Wicker R B 2009 Microstructures and mechanical properties of electron beam-rapid manufactured Ti–6Al–4V biomedical prototypes compared to wrought Ti–6Al–4V *Mater. Charact.* **60** 96-105

[5] Wang F, Williams S and Rush M 2011 Morphology investigation on direct current pulsed gas tungsten arc welded additive layer manufactured Ti-6Al-4V alloy *Int. J. Adv. Manuf. Technol.* **57** 597-603

[6] Martina F, Mehnen J, Williams S W, Colegrove P and Wang F Investigation of the benefits of plasma deposition for the additive layer manufacture of Ti–6Al–4V *J. Mater. Process. Tech.* **212** 1377-1386

[7] ANSYS17.2 2016© *ANSYS Inc. Canonsburg Pennsylvania (USA)*

[8] Nikam S H and Jain N K 2017 Three-dimensional thermal analysis of multi-layer metallic deposition by micro-plasma transferred arc process using finite element simulation *J. Mater. Process. Tech.* **249** 264-273

[9] Alimardani M, Toyserkani E and Huissoon J P 2007 Three-dimensional numerical approach for geometrical prediction of multilayer laser solid freeform fabrication process *J. Laser Appl.* **19** 14-25

[10] Mills K C 2002 *Recommended values of thermo-physical properties for selected commercial alloys* (Cambridge: Woodhead Publishing series) p 211

[11] Nikam S H and Jain N K 2018 3D-finite element simulation and image processing based prediction of width and height of single-layer deposition by micro-plasma-transferred arc process *Int. J. Adv. Manuf. Technol.* 10.1007/s00170-017-1472-x